SEISMIC RESPONSE OF LINEAR, FLANGED, AND CONFINED MASONRY SHEAR WALLS

M. T. Shedid[1], W. W. El-Dakhakhni[2], and R. G. Drysdale[3]

[1] *Ph.D. Candidate, Dept. of Civil Engineering, McMaster University, Hamilton. Ontario, Canada*
[2] *Assistant Professor, Martini Mascarin and George Chair in Masonry Design, Dept. of Civil Engineering, McMaster University, Hamilton. Ontario, Canada*
[3] *Professor Emeritus, Dept. of Civil Engineering, McMaster University, Hamilton. Ontario, Canada*
Email: shedidmmt@mcmaster.ca, eldak@mcmaster.ca, drysdale@mcmaster.ca

ABSTRACT:
A potentially limiting feature of reinforced masonry shear walls is the presence of a single line of vertical reinforcement along the wall length that cannot be effectively tied to delay buckling. Especially under cyclic loading, when opening and closure of wide cracks occurs, compression closure of the previous tension cracks causes all of the compressive stresses to be carried by isolated bars at the crack location. This situation affects the stability of the compression zone and may lead to out-of-plane buckling of the wall or local buckling of the reinforcement, which can lead to an accelerated degradation in strength due to increased damage. This limitation may be avoided by using boundary elements at the end zones of the walls or by structurally connecting a linear wall to an intersecting wall which would limit the damage at the end zone of the wall, provide out-of-plane stability for the end of the wall, and delay buckling of the vertical bars. The experimental data presented is the first phase of an investigation of the response of flexural concrete masonry shear walls with various geometries at the ends of the walls. The conditions studied are the effects of structurally connecting a flange to a linear reinforced masonry shear wall and of creating a boundary element at each end of the wall. The walls were tested under reversed lateral cyclic displacement simulating earthquake excitation. Details of the linear, flanged, and confined wall tests are presented in this paper. In general, high levels of ductility accompanied by relatively small strength degradation were observed for the test specimens with significant increase in ductility for the flanged and confined walls.

KEYWORDS: Flanged Walls, Boundary Elements, Ductility, Reinforced, Masonry, Earthquake.

1. INTRODUCTION

Recent examples of large loss of life and huge economic impact due to damage and even complete collapse of buildings due to earthquake loading have led to adoption of more stringent seismic design requirements in North America. This is particularly true for low and moderately active seismic regions and has especially affected design of masonry buildings which are perceived to have less ductility and be more vulnerable to seismic loading.

A widely held belief is that masonry cannot provide high ductility. However, the results of recent experimental research at McMaster University (Shedid 2006, Long 2006), and in other parts of the world (Abrams 1986), show that this is not true. High ductility and low degradation of strength under cyclic loading can be achieved for reinforced masonry shear walls failing in flexure. The lateral load capacity of reinforced masonry shear walls is also found to be maintained for drift levels beyond those corresponding to maximum load, with almost no degradation of lateral load capacity even after toe crushing and spalling of the face shells of the end blocks has occurred. It is only after splitting of the outermost grout column and buckling of the end reinforcing bars have occurred that strength degradation becomes significant. In this regard, a masonry shear wall having a single line of vertical reinforcement has almost no confinement for the compression zone. Such masonry shear walls may be vulnerable to buckling of the vertical bars in compression and out-of-plane buckling during reversed cyclic loading (Paulay and Priestley 1993). Hence, confinement of the ends of the walls is a strategy

that is expected to delay splitting of the grout column and buckling of the end bars and, therefore, should increase the displacement ductility by delaying strength degradation.

The behavior for three fully grouted reinforced masonry shear walls is presented to document the effects of different end configurations on the inelastic behavior and ductility of masonry walls under seismic loading.

2. EXPERIMENTAL PROGRAM

Although a fairly large amount of experimental testing has been conducted on linear reinforced masonry walls, relatively little data is available on reinforced masonry walls with flanges or with boundary element at the wall ends. The reported tests were designed to investigate the cyclic flexural response of linear reinforced concrete masonry walls, walls with flanges, and walls with boundary elements. The tests were designed to investigate the enhancement of ductility through larger curvatures and increased stability of the compression zone as a result of attaching flanges and boundary elements to linear walls. All walls were subjected to fully reversed displacement-controlled quasi-static cyclic loading and were loaded up to 50% degradation of strength in order to obtain information on the post-peak behavior.

2.1. Material Properties

Type S mortar, with an average flow of 125% was batched by weight with proportions of Portland cement: Lime: Dry sand: Water = 1.0: 0.2: 3.5: 0.9. Fine grout mixed in the laboratory was used for grouting the walls. The average cylinder compressive strength of the grout was 21.8 MPa (*c.o.v. = 15.7%)*. Grout filled 4-block high prisms were constructed in running bond to determine the wall properties. The average compressive strength of the grouted masonry prisms, f'_m, was 16.3 MPa (*c.o.v. = 14.3%)*. Tensile tests conducted on the vertical reinforcement gave an average yield strength of 496.3 MPa (*c.o.v* = 2.3%). The concrete used in the wall foundation had an average compressive strength of 27.3 MPa (*c.o.v*. = 2.8%). Concrete mixed in the laboratory, having an average compressive strength of 36.0 MPa (*c.o.v. = 7.6%),* was used in the three slabs representing storey levels.

2.2. Wall details and construction

For a typical 5 storey masonry building, wall lengths between 2 m to 8 m long result in an aspect ratio of at least 1.5 (storey height is about 2.4 m), and axial compressive stress can vary from about 1 MPa to 2 MPa (0.2 to 0.4 MPa per floor). The design of the initial phase of this research was based on the stated range of aspect ratios and axial compressive stress.

Laboratory testing of full-scale masonry walls can be impractical due to space limitations, construction and testing constraints, and time and financial restrictions. Even with the 12 m head room and the strong floor in McMaster's Applied Dynamics Laboratory, large full-scale structures cannot be built and tested. An alternative solution was to model full-scale elements using half-scale masonry units that have shown to closely simulate full scale construction (Long 2006). A reasonable and safe specimen height to be tested in the laboratory was estimated to be about 4.0 m. Therefore, when using half-scale blocks, the corresponding number of stories to model is 3, assuming that the floor height to be about 1.2 m (2.4 m in full-scale construction). The wall length was then selected to be 1.8 m containing 19 cells which allowed for many possible arrangements of vertical reinforcement, such as every cell, every other cell, and every third cell. Based on the previous values, the wall dimensions were selected to be to 1.80 m long × 3.99 m high (representing about 3.6 m× 8.0 m in full scale construction) which result in an aspect ratio of 2.2.

The construction of the test walls started with construction of the reinforced concrete base. Then construction of a wall up to a storey height was followed by grouting the wall solid before construction of the reinforced concrete slab representing the storey floor. An experienced mason constructed all of the walls in running bond

with the half-scale hollow concrete masonry units using face shell mortar bedding and 5 mm mortar joints. The length of the walls consisted of nine and half concrete half-scale blocks, and the height of the walls consisted of 39 courses (13 courses per storey) and 3 reinforced concrete slabs (each 100 mm thick). All specimens were fully grouted and the vertical and horizontal reinforcement were uniformly distributed over the wall. The three concrete slabs were reinforced in two orthogonal directions and were cast at wall heights representing the floor of each storey. The slabs extended the whole length of the wall and extended laterally 150 mm from each side of the wall.

The configurations of the three test walls and details of the vertical reinforcement are shown in Fig. 1. Wall 1 was a linear wall and was heavily reinforced with 19 No. 10 vertical bars (A_s = 100 m^2/bar) along the length (ρ_v = 1.17%). The web of the flanged wall (W2) was 90 mm thick (1 wythe) and the flanges were composed of an additional half block extending from each side of the wall at each end to increase the end thickness to 285 mm instead of 90 mm for a length of 90 mm. The wall was reinforced with 5 No. 10 vertical bars along the web and 3 No. 10 bars in each flange (ρ_v = 0.56%). The web of the wall with boundary elements (W3) was 90 mm thick and the boundary elements were composed of an additional block at each wall end which increased the end thickness to 185 mm instead of 90 mm for a length of 185 mm (1 block). The wall was reinforced with 3 No. 10 vertical bars along the web and 4 No. 10 bars in each boundary element (ρ_v = 0.56%).

The horizontal reinforcement in the walls, consisting of D4 wires (25.4 mm^2), was placed in the notch located in the webs of the blocks. The presence of this 20 mm deep notch provided some continuity of the grout by forming a bond beam and fully encasing the wires as was visible after spalling of the face shells. The horizontal reinforcement in the linear walls formed 180° hooks around the outmost vertical reinforcement. The 200 mm return leg of the hook extended to the third last cell, as shown in Fig. 1 (a), to provide adequate anchorage. Otherwise, in the case of the walls with boundary elements, the horizontal reinforcement was anchored inside the boundary element where closed ties were provided around the 4 end bar arrangement as shown in Fig. 1 (c). A similar anchorage of the horizontal reinforcement was used for the wall with flanges; the horizontal bars from the web were anchored in the flanges in addition to another 200 mm length of bar, as shown in Fig. 1 (b).

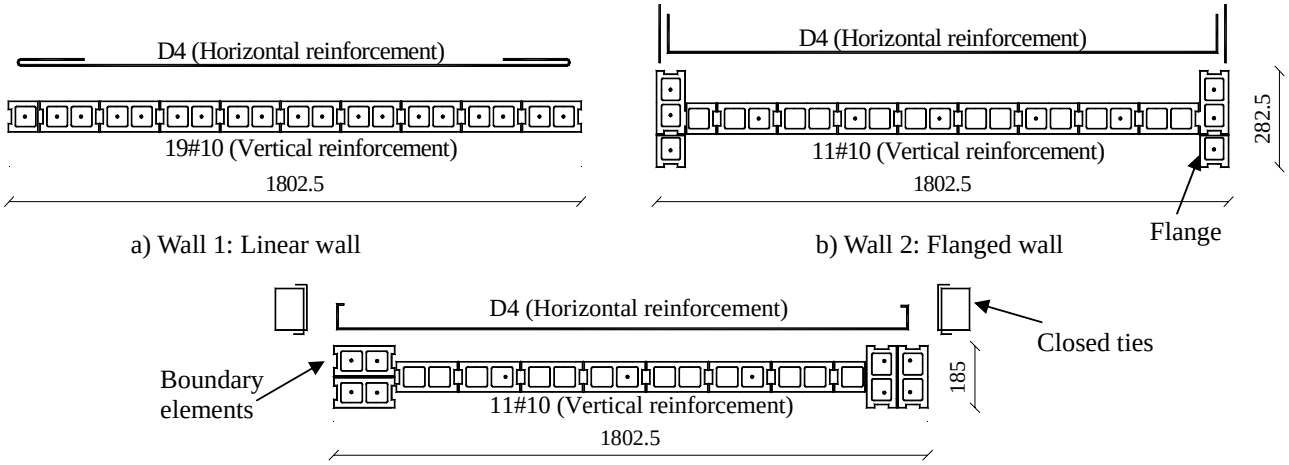

a) Wall 1: Linear wall

b) Wall 2: Flanged wall

c) Wall 3: Confined wall

Figure 1 Details of cross section and reinforcement in the test walls

The reinforcement ratios, number of bars, and level of applied axial stress for the test walls are listed in Table 2.1. Walls 1, 2, and 3 had vertical steel ratios of 1.17%, 0.55% and 0.55% respectively, and were subjected to axial compressive stresses, including the self weights of the walls, of 1.09 MPa, 0.89 MPa, and 0.89 MPa, respectively. These walls were designed to have the same lateral load capacity at ultimate masonry compressive strain while being subjected to the same magnitude of axial compressive load. This criterion was selected to illustrate the change in the performance if a linear wall in a structure was replaced by a wall with flanges or boundary elements while designed for the same loads.

Table 2.1 Summary of wall details

Specimen designation	Wall dimensions	Vertical reinforcement		Horizontal reinforcement		Axial stress (MPa)
		Number of bars and bar size	ρ_v (%)	D4 wire @	ρ_h (%)	
W1	1802 mm × 3990 mm (Length × Height)	19 # 10	1.17	190 mm	0.15	1.09
W2		11 # 10	0.55	190 mm	0.15	0.89
W3		11 # 10	0.55	190 mm	0.15	0.89

2.3. Test Setup

The test rig was designed to test shear walls up to three meters long under reversed cyclic loading. As shown in Fig. 2, the rig consisted of a 4200 mm long × 1100 mm wide × 600 mm deep reusable concrete floor slab that was prestressed to the structural floor with the aid of ten, 63 mm diameter, post-tensioned steel bolts spaced at 920 mm in both the longitudinal and transversal directions. Sixteen 25.4 mm diameter steel prestressing bars were anchored in the reusable floor slab and, after positioning the test wall, were post-tensioned to clamp the wall base to the reusable floor slab in order to prevent its rotation during wall testing. These prestressing bars were spaced at 400 mm in the longitudinal direction and at 320 mm in the transverse direction.

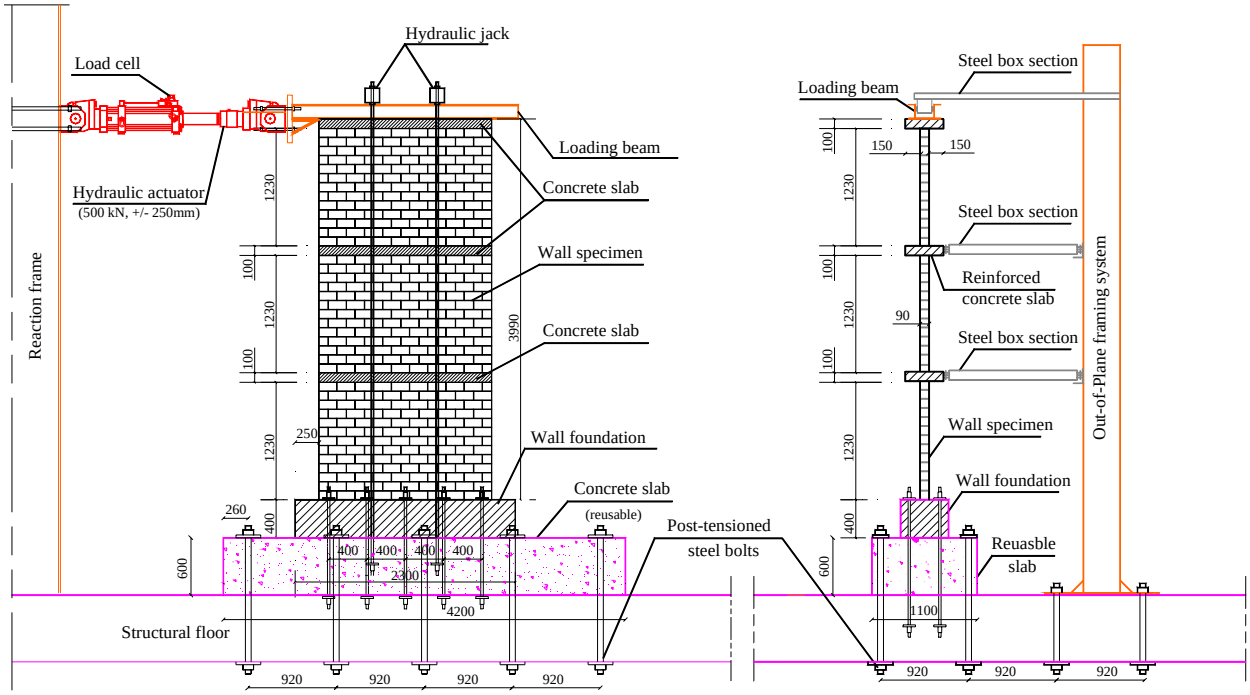

Figure 2 Test setup

Axial load was applied to the top of the wall by means of four 13 mm diameter high strength prestressing rods anchored to an HSS 102×102×4.8 beam that was attached to the reusable concrete slab. Each pair of bars pivoted on a roller oriented along the length of the wall. Load was applied by a manually operated hydraulic jack on one side of each pair of the prestressing bars. Load was distributed along the wall length through the top steel loading beam. The lateral cyclic load was applied using an MTS hydraulic actuator positioned to coincide with the top of the wall in order to create a zero moment condition at the top of the wall. The actuator was attached to the stiff steel loading beam at the top of the walls to which the vertical reinforcement of the wall was welded. Steel dowels (No. 10) were inserted, during grouting of the second half of the 3rd storey, in all the cells not containing vertical reinforcement. These dowels extended into the 2 top masonry courses and to a height of

200 mm above the top course and were then welded to the top beam in the cells not containing vertical reinforcement. This arrangement was selected to uniformly transmit the lateral load along the whole length of the wall instead of as a point load at the top corner of the wall.

The walls were braced against out-of-plane displacement using two hollow steel link members pinned to a steel frame and connected to each reinforced concrete slab representing the storey floor, as illustrated in Fig. 2. The box sections were attached to the out-of-plane bracing frame and to the reinforced concrete slab at each storey with 25 mm high strength threaded rods to create pinned connections. The two link members at each storey were designed to offer minimal resistance to the in-plane displacement of the loading beam and to prevent out-of-plane movement of the wall at the first and second stories during the test. The top bracing system was different and consisted of rollers attached to the box section bracing members between the 2 channel sections of the loading beam to offer minimal resistance to the in-plane movement.

2.4. Instrumentation and Test Procedure

Thirty-six potentiometers were used to monitor lateral deflections, vertical deformations, diagonal deformations, slip along the base, and wall uplift. The vertical displacements of the walls were monitored by the potentiometers installed vertically along the wall ends. Each of these potentiometers measured the vertical movement of the storey relative to the concrete slab beneath it and was used to calculate average curvature over that segment of the wall height. The lateral displacements of the wall at different heights were measured by seven horizontally positioned potentiometers. In addition, electrical strain gauges were epoxied to the reinforcing steel bars prior to wall construction. The gauges were located within the most highly stressed region to monitor initial yielding, extent of yielding over the wall height, and penetration of yielding inside the foundation. Eight strain gauges were used in the linear wall and sixteen gauges were used in the walls with flanges or boundary elements. The strain gauges were located at the same heights for all walls.

A displacement controlled loading procedure was used until yielding of the outermost bar had occurred based on the reading of the strain gauges attached to the bar at the interface between the wall and the foundation. The initial displacement cycles were based on reaching 0.2, 0.4, 0.6, 0.8 and 1.0 times the theoretical yield resistance of the wall, which was within 5% of the measured resistance based on the readings of the strain gauges. Then for subsequent displacement cycles, the walls were tested using increments equal to multiples of the displacement recorded at the onset of yielding of the reinforcement, Δ_y.

3. EXPERIMENTAL RESULTS

For each specimen, cracking and progressive failure observations, as well as the hysteresis loops are presented. Load-displacement response of the wall is then discussed.

3.1 Wall 1: Linear Wall

The hysteresis loops for Wall 1, shown in Fig. 3, indicate a symmetric response for loading in both directions. The slopes of the loops decreased gradually with increases in lateral top displacement indicating loss of stiffness. The response of the wall was almost linearly elastic characterized by thin hysteresis loops generating low energy dissipation up to the first yield of the outermost reinforcement at the base of the wall. At higher displacement levels, larger loops indicated higher amounts of energy dissipation associated with increases in plastic deformations. Yielding of the outermost reinforcement was recorded at 101 kN and 7.9 mm displacement for loading in the (+) direction, and at 110 kN and 9.0 mm displacement for loading in the (-) direction. The wall was loaded based on a yield displacement equal to 8.5 mm.

During the loading cycle, which corresponded to initial yielding of the outermost vertical reinforcement, horizontal cracks were seen along all bed joints in the first storey and along the first and second bed joint in the second storey whereas no cracks were seen in the third storey. Diagonal cracks were observed over the full height of the first storey along the middle third of the wall length during the 25.5 mm ($3\times\Delta_y$) loading cycle and

extended to the second storey but were concentrated over the lower six courses above the concrete slab. Diagonal cracks in the second storey became stepped over the first two courses above the concrete slab and extended through the concrete slab to join with the diagonal cracks in the lower storey.

As shown from the hysteresis loops for loading in the (+)ve direction, Wall 1 reached a maximum lateral load capacity of 177 kN at 25.5 mm ($3\times\Delta_y$) top lateral displacement. The wall had lost about 7% and 10% of its maximum lateral capacity at 34.0 mm ($4\times\Delta_y$) and 42.5 mm ($5\times\Delta_y$) top lateral displacements, respectively. During the second loading cycle corresponding to $5\times\Delta_y$, the wall had lost about 29% of its maximum lateral load capacity, which coincided with splitting of the outermost grout column and buckling of the outermost reinforcement. The wall, when displaced to 51 mm ($6\times\Delta_y$) had lost about 40% of its maximum capacity, and, at this level, buckling of the outermost three vertical bars was observed and was associated with crumbling of the grout columns encasing these bars. During loading in the (-)ve direction, Wall 1 reached a maximum lateral load capacity equal to 180 kN at $3\times\Delta_y$ top lateral displacement. The wall had lost about 5% of its maximum lateral capacity at the first $5\times\Delta_y$ top lateral displacement. During the second loading cycle, the wall had lost about 17% of its maximum lateral capacity, which coincided with splitting of the outermost grout column and buckling of the outermost bar. When displaced to 51 mm ($6\times\Delta_y$) in the (-)ve direction, the wall had lost about 24% of its maximum capacity and, at this level, buckling of the outermost vertical bar was observed and was associated with crumbling of the grout columns encasing this bar.

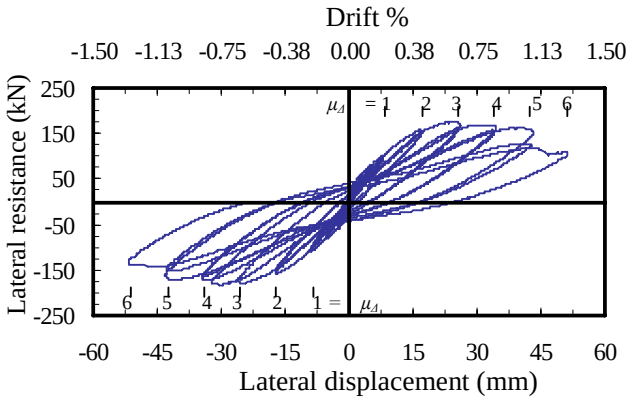

Figure 3 Hysteresis loops for Wall 1

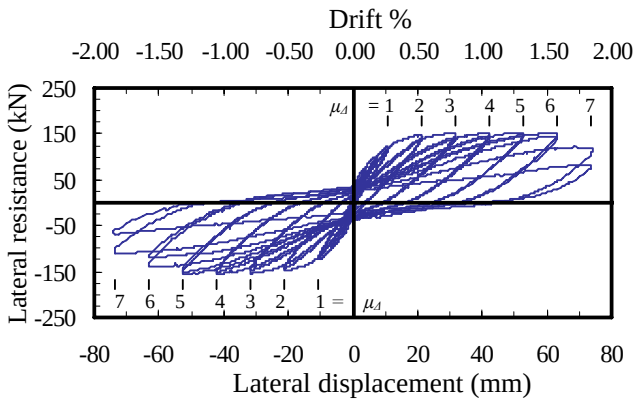

Figure 4 Hysteresis loops for Wall 2

3.2 Wall 2: Flanged Wall

The hysteresis loops for Wall 2, shown in Fig. 4, indicate a symmetric response for loading in both directions similar to Wall 1. Yielding of the outermost reinforcement was recorded at 121 kN and 10.8 mm displacement for loading in the (+) direction, and at 123 kN with 10.3 mm displacement for loading in the (-) direction. The displacement increments for loading were based on a yield displacement equal to 10.5 mm.

As shown from the hysteresis loops, Wall 2 reached a maximum lateral load capacity of 152 kN at 31.5 mm ($3\times\Delta_y$) top lateral displacement during loading in the (+)ve direction. The wall did not loose any significant amount of lateral capacity until 63 mm ($6\times\Delta_y$) top lateral displacement. The wall had lost about 20% and 50% of its maximum lateral capacity during the first and second cycles at 73.5 mm ($7\times\Delta_y$) top lateral displacement, respectively. The significant loss in strength coincided with splitting of the outermost grout columns encasing the three vertical bars in the flange and buckling of this reinforcement.

During loading in the (-)ve direction, Wall 2 reached a maximum lateral load capacity of 155 kN at $3\times\Delta_y$. The wall had lost about 10% of its maximum lateral capacity during the first cycle at $6\times\Delta_y$ and during the second loading cycle, the wall had lost about 22% of its maximum lateral capacity. This coincided with splitting of the outermost grout column and buckling of the outermost reinforcement. At $7\times\Delta_y$ displacement in the (-)ve direction, the wall had lost about 30% of its maximum capacity. At this level, buckling of two vertical bars in the flange and crumbling of the grout columns encasing these bars were observed.

3.3 Wall 3: Confined Wall

The hysteresis loops for Wall 3, shown in Fig. 5, indicate a symmetric response for loading in both directions. Yielding of the outermost reinforcement was recorded at 110 kN and 9.0 mm displacement for loading in the (+)ve direction, and at 106 kN and 9.4 mm displacement for loading in the (-)ve direction. The increased displacement for each cycle was based on a yield displacement of 9.2 mm.

As the hysteresis loops show, Wall 3 reached a maximum capacity equal to about 152 kN at 36.8 mm ($4\times\Delta_y$) top lateral displacement. The wall did not loose any significant amount of lateral capacity until 92 mm ($10\times\Delta_y$) top lateral displacement, but during the second loading cycle at this displacement, the wall lost about 15% of its maximum lateral capacity. Unfortunately, as can be seen, this is likely due to having accidentally loaded the wall to a top displacement of 124 mm instead of 92 mm at the beginning of the cycle. The 124 mm displacement (more than $13\times\Delta_y$) was imposed without loss of capacity but did cause additional yielding of the tension bars which affected subsequent cycles of loading At the 92 mm displacement level, crumbling of the unconfined grout column (outside of the ties) occurred over the lower course and the vertical reinforcement buckled between the base of the wall and the first confining tie located at 80 mm above the base. A significant loss in strength occurred during loading to a target displacement of 101.2 mm ($11\times\Delta_y$) due to fracture of the vertical reinforcement which is likely is due to low cycled fatigue. The data from the accidental loading to a top displacement of 124 mm indicates that the wall would have produced even higher ductility capabilities than shown if fewer cycles of loading had been applied at lower displacement levels to reduce the fatigue effect.

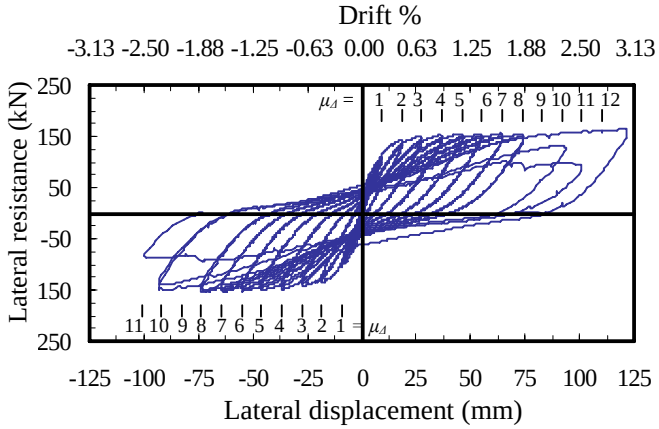

Figure 5 Hysteresis loops for Wall 3

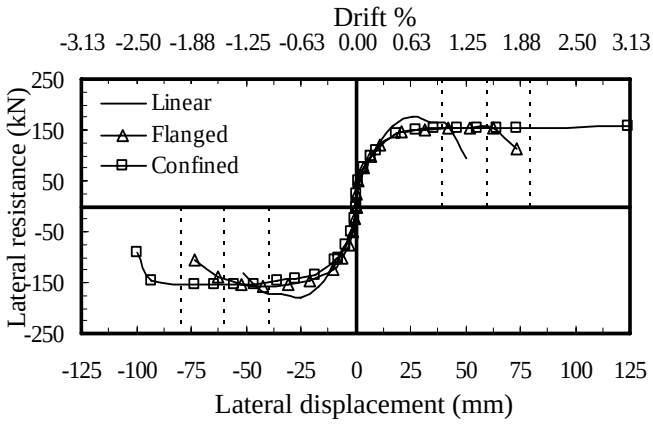

Figure 6 Load-displacement relationships

3.4 Load-Displacement Relationships and Extents of Damage

The envelopes of the load-displacement loops for the three walls are shown in Fig. 6. The enhanced displacement and ductility capabilities are obvious when comparing the test walls. The heavily reinforced linear wall had good ductility but significantly less than the other two with the confined wall exhibiting a displacement ductility of at least 10. The linear wall lost about 10% of its lateral resistance when loaded to displacements beyond $4\times\Delta_y$. A similar loss in strength for the flanged wall was not seen until the $6\times\Delta_y$ displacement was applied. The outstanding performance of the confined wall is clearly seen from the figure as the wall reached $10\times\Delta_y$ cyclic displacement with no strength degradation. The corresponding drift levels ranged from about 1% for the linear wall to 2% for the confined wall. In this regard, it should be noted that the same strain levels applied to longer walls would result in proportionally less drift but equal ductility.

The test results show the significant enhancement of the displacement and ductility capabilities to a linear wall by just adding a half block with one grouted and reinforced cell at each side of the wall. Even without special detailing of the horizontal reinforcement to confine the grout and control buckling of the vertical reinforcement in the flange. The increased thickness of the wall at the ends resulted in an outstanding performance of the wall characterized by

significant increase in lateral displacement and limited damage localized at the toe of the wall until failure occurred, as shown in Fig. 7. The confined wall provided a similar benefit and the added benefit of having ties brace the enclosed end bars to delay their buckling and confine the grouted section within the reinforcing cage.

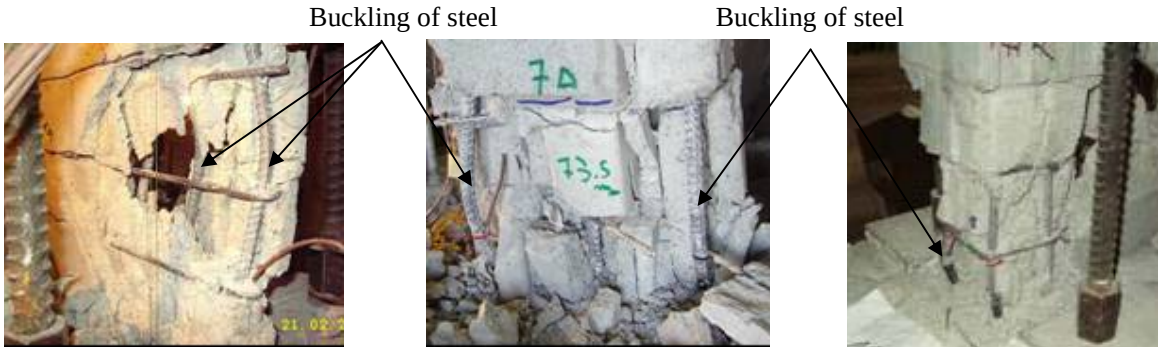

Wall 1: Linear wall | Wall 2: Flanged wall | Wall 3: Confined wall

Figure 7 Extents of damage near the end of the test

The addition of floor slabs was a departure from previous testing (Shedid 2006). In this regard, it was observed that cracking was more concentrated in the region between the foundation and the first concrete slab for all test walls. Minor cracks were seen between the first and the second concrete slabs, and almost no cracks were seen above the second slab. Future research will evaluate any differences resulting from the presence of floor slabs.

4. CONCLUSION

The substantially improved performance of the flanged and confined walls was achieved through the addition of one block at each end of the wall. This cost would be much more than offset by the elimination of 8 of the 19 bars used in the linear wall. It is suggested that these end geometries can be added to masonry construction with minimal impact on architectural or construction practices.
The reported test results demonstrate the high ductility and energy dissipation potential of reinforced masonry. There is an urgent need for this information to be incorporated in building codes.

5. ACKNOWLEDGMENT

The financial support of the McMaster University Centre for Effective Design of Structures (*CEDS*) funded through the Ontario Research and Development Challenge Fund (*ORDCF*) is greatly appreciated. Provision of mason time by Ontario Masonry Contractors Association and Canada Masonry Design Centre is appreciated. The supply of half-scale blocks by the Canadian Concrete Masonry Producers Association is gratefully acknowledged.

6. REFERENCES

Abrams, D., (1986), Measured hysteresis in a masonry building system. Proceedings of the third U.S. Conference on Earthquake Engineering, Charleston, South Carolina, August.

Drysdale, R., and Hamid, A. (2005). Masonry structures- behaviour and design. First Canadian Edition, Canada Masonry Design Centre, Mississauga, ON, Canada.

Long, L. (2006). Behaviour of half-scale reinforced concrete masonry shear walls. M.A.Sc. Thesis, Department of Civil Engineering, McMaster University, Ontario, Canada.

Paulay, T., and Priestley, M., (1993). Stability of ductile structural walls. *ACI Structural Journal*, **(90)4**, 385-392.

Shedid, M. (2006). Ductility of reinforced concrete masonry shear walls. M.A.Sc. Thesis, Department of Civil Engineering, McMaster University, Ontario, Canada,.